Universidad Politécnica de Cartagena
E.T.S. de Ingeniería de Telecomunicación

Espacio-Tele□o n^{0}1 (2010)
Revista de la ETSIT-UPCT

Human Head Natural Protection Against Electromagnetic Fields

Miguel A. García-Fernández,
Juan F. Valenzuela-Valdés y David Sánchez-Hernández

Departamento de Tecnología de la Información y las Comunicaciones.
Universidad Politécnica de Cartagena.

garciafernandez.ma@upct.es; juan.valenzuela@upct.es;
david.sanchez@upct.es

Abstract

In this paper we provide concluding evidence that the human skull acts as a dynamic barrier to electromagnetic fields (EMF) and temperature flow at 1800 MHz. This natural helmet effectively and dynamically protects brain tissue against safety-defined threshold temperature increase due to external EMF induction. A half-wavelength dipole antenna has been employed as the EMF source. The human head is modelled by several coronal planes extracted from the Visible Human Project. Results described here have a great importance should thermal effects be directly used to derive basic restrictions to EM fields safety limits for human exposure.

Project/Group: Microwave, Radiocommunications and Electromagnetism Engineering Group (GIMRE). Supported by: FUNDACIÓN SENECA. Plan de Ciencia y Tecnología de la Región de Murcia. Código: 05746/PI/07.

Subject Research: *Biological effects of electromagnetic radiation; Dosimetry*; *Occupational health and safety; Specific absorption rate (SAR), Temperature.*

1. Introduction

The emergence of mobile phone communications has triggered the necessity to redefine safety limits regarding the human exposure to EMF in the near-

field regime and the need to define accurate evaluation procedures [1], since a human body exposed to excessive electromagnetic fields may suffer from temperature increments which could pose a health treat. An increase of more than 1^oC in any part of the brain will bring heat exhaustion or even a heat stroke [2] and an increase of 0.2-0.3^oC in the hypothalamic region would alter thermoregulatory behaviour [3]. Evaluating compliance to safety limits is usually accomplished by measuring SAR, but in fact, it is now clear that SAR alone may not provide an adequate description of the regional thermal environment [4]. Even though the dielectric properties of the phantom liquid or gel are normally averaged over those of a more realistic heterogeneous model [5], arbitrary correction factors have been proposed [6]. These correction factors have already been demonstrated to be erroneous for typical GSM base station antennas [7]. In addition, a recent paper [8] has shown that the human exposure to electromagnetic fields from a base station antenna using a realistic heterogeneous model is a problem that strongly depends upon specific human tissue structure being exposed and antenna topology. This makes a solo simple factor not possible for an accurate description of the problem when using homogeneous models. In consequence, and due to the recent availability of powerful computers, the direct calculation of thermal thresholds with EMF exposure has recently received considerable attention [9]. To tackle this aspect of EMF exposure more realistic and therefore complex models have been developed based on the conjunction of Maxwell equations, thermal diffusion theory and human biological data. Effectively, the human head is represented as a multi-layer model where each layer corresponds to different kind of human tissue with its own thermal and electromagnetic characteristics. Above these refinements, a thermoregulatory model is also typically employed to approach real exposure scenarios as much as possible. In this work it has been demonstrated that the human skull acts as a protecting shield against EMF in the near-field regime at 1800 MHz. This protection helps avoiding thermal damage of sensible brain tissues, keeping the subject safe to overheating processes. The protective nature is performed by the combination of tissue layers and the specific position and thermal characteristics of the skull.

2. Methods and Models

The electrical and thermal properties of the employed tissues have been extracted from the literature [10]. The employed biological data is reproduced in Table 1. The relevant 2D representations of the human head are some coronal planes extracted from the Visible Human Project, as depicted in Figure 1. For definiteness and reproducibility we have employed as the near-field source the EMF produced by a half-wavelength dipole antenna at 1800 MHz. The power radiated by the dipole was modified so as to provide a maximum temperature increase of 0.2^oC in the brain. The above is done in two different time scales corresponding to exposures of 6 and 30 minutes. In order to analyse the efficiency of the whole skull, many different head regions have been considered.

Tissue	ε_T	σ	ρ	C	K	A	B
Blood	59.37	2.044	1058	3840	0.49	0	0
Blood Vessel	43.34	1.066	1040	3553	0.46	1600	9000
Bone (Cancellous)	19.34	0.588	1920	2150	0.30	2510	14120
Bone (Cortical)	11.78	0.275	1990	1650	0.30	0	0
Bone (Marrow)	5.37	0.069	1040	2700	0.22	5020	28230
Brain (Cerebellum)	46.11	1.709	1038	3687	0.57	10040	56490
Brain (Gray Matter)	50.08	1.391	1038	3687	0.57	10040	56490
Brain (White Matter)	37.01	0.915	1038	3600	0.50	2820	15890
Skin	38.87	1.845	1125	3610	0.42	2190	12310

Table 1: Font Sizes for Papers. *σ:(S/m), ρ: Density (Kg/m^3), C: Specific heat capacity (J/Kg^oC), K: Thermal conductivity (W/m^oC), A: Metabolic heat production (W/m^3), B: Blood flow associated term ($W/m^{3o}C$).*

However and since we found the same overall behaviour in all the different points we have analyzed, we have chosen to show data only from the top cranial and right temple scenarios, which are depicted in Figure 1.

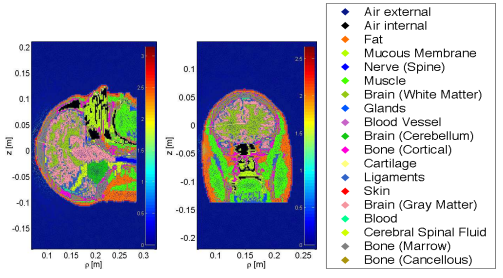

Figure 1: Top-cranial slice (left), right temple slice (middle) and legend of tissues (right), from the Visible Human Project, used in the simulations.

The distance between the antenna and the human head is fixed once and for all to 0.45λ. At this distance the heterogeneous human head model matches the dipole antenna impedance in the initial setting. This causes a considerable SAR and temperature increase. All analyses were performed by using an in-house software code, prepared in combination to the Partial Differential Equation (PDE) Toolbox in MATLAB. A human thermoregulatory model was also programmed following the bio-heat equation, and it is a refinement of the original model used by Pennes [11]. This differential equation incorporates electromagnetic and heat diffusion data applied to human tissue by:

$$\rho \cdot C \cdot \frac{\partial T}{\partial t} = \nabla \cdot (K \cdot \nabla T) + \rho \cdot SAR + A + B \cdot (T_b - T)\,, \qquad (1)$$

where C is the specific heat capacity, K is the thermal conductivity, ρ is mass density of the tissue, A is the metabolic heat production, B is the heat-sink strength, T_b is the blood temperature, t is time and T is the temperature. SAR is calculated using the well-known equation,

$$SAR = \frac{\sigma \cdot E^2}{\rho}, \tag{2}$$

where σ is the electrical conductivity of the tissue and E is the root mean square (RMS) value of the electric field. The above set of equations is fed with the necessary boundary data by:

$$K \cdot \hat{n} \cdot \nabla T = H \cdot (T_r - T)\,, \tag{3}$$

where ($\hat{n}$, H, T_r) stand for the normal unit vector to the boundary of the human head, the environment heat transfer coefficient and the room temperature respectively. Due to 2D characteristics of the PDE toolbox, ϕ-symmetry is employed to solve the EM field, which is accurate enough for a dipole antenna as the exciting source. The centre of the dipole was settled as the origin of coordinates. After SAR is calculated, temperature increase is evaluated for all tissues by solving the modified bio-heat equation (1), where T_b is set to 37 ^{o}C. Boundary conditions were established with H equal to 7 $W/(m^{2}\cdot^{o})$ and a room temperature of 23 ^{o}C. The room temperature was chosen to follow within the thermopreferendum region. In this region a sedentary light-dressed man feels comfortable with no air flows. The in-house thermal model includes heat diffusion and convection, metabolic heat production and heat-sink from tissue volume by blood perfusion. Thermoregulatory control can be achieved in the head model in real time, which can keep a constant temperature under no RF exposure being slightly altered by the heat loss in body surface due to intimate contact to air. Thermal conditions in this contribution are kept just under the vasomotor adjustment, that is, just under the lower critical temperature (LCT) [12]. This facilitates the use of basal metabolism as adequate. In this way, no vaporization is evaluated and harsh electromagnetic exposure is out of the scope for this contribution, that is, mass transfer and their associated heat-transfer mechanisms are avoided. Once the coronal plane is identified and we have the corresponding temperature increase on any point of it, we localized the spot in the brain of maximal increase of temperature p. Then, we define our line of measurements $\bar{c}\bar{p}$ as the line that begins at the geometrical centre of the brain c and passes through p ending on the aerial region. Our simulated results and data are displayed along this linear axis. In this way, given a particular antenna-head configuration, we define a particular axis that passes throughout the point of maximum heating that permit us to control the most vulnerable part of the brain.

3. Simulated Results

In this paper, results are expressed in terms of minimal power delivered and associated SAR required to produce the aimed maximum local increment of brain tissue of 0.2 ^{o}C in different scenarios. In addition, different figures of local temperature increment along the different tissues of the brain are provided. To test our working hypothesis, i.e. that the skull acts as a thermal-EM helmet, we probed the human head to the radiation of the dipole antenna from different positions in the vicinity of the head. Following the procedure described in the previous section, we obtained the increase of temperature along the $\bar{c}\bar{p}$ axis for each one of the different configurations under study. The above is simulated for short and long exposure corresponding to 6 min. and 30 min., respectively. In this way, we have devised a procedure to capture the strength of the natural shield protecting the head at the diverse time averaging periods defined in the standards worldwide. Results for the cranial and temple regions are depicted in Figures 2 and 3, respectively. From these figures it is clear that almost no thermal fluctuations or SAR leek into the inner brain. Most of the energy absorbed by the head is localized in the outer region outside the skull. As expected, the time dependence of the above phenomena shows a conformal behaviour, since only the relative power needs to be re-scaled to recover the correct curves. This reinforces our aim to maintain the experiments just below the LCT region. The above response to EMF exposure of the human head is also reproduced in other geometrical settings around the head, which are not depicted here for brevity. Results show that the outer layers of the human head constitute a built-in shield which acts as a dynamical barrier, scattering thermal fluctuations and EMF away from the brain back to the external regions. In this dynamical process the un-scattered thermal fluctuations and the EMF that reach the brain tissue are really subdominant, where the ratio of scattered to transmitted thermal fluctuations is only of order 10^{-3}.

In this article we have used a realistic human head model exposed to EMF in the near-field region employing a hybrid framework based on electromagnetic field theory, heat transport theory and thermoregulatory response of the human body. In the above data analyses, it is not difficult to identify the location of this natural shield as the region where the thermal fluctuations and EMF decay abruptly. In all performed simulations, we found that this region corresponds to the location of the skull or its natural continuation. This corresponds to the region delimited by the vertical brown or pink lines in Figure 2 and 3. In consequence, it can be observed that the principal component of the natural shield is indeed the skull properties and the specific position of the skull within the multilayer tissue structure.

4. Conclusions

The specific position and properties of the skull within the human head have been identified to act as a protective garment, avoiding external electromagnetic fields and their associated thermal increase getting into the inner brain. This has been found to happen regardless the power delivered when the room temperature is just below the LCT, that is, under the vasomotor adjustment with no sweating.

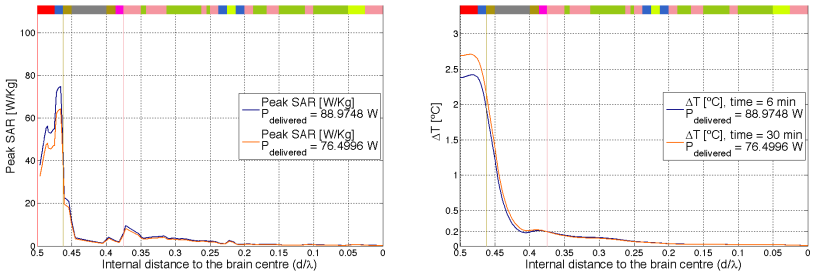

Figure 2: SAR (up) and temperature increase (down) for the cranial setting.

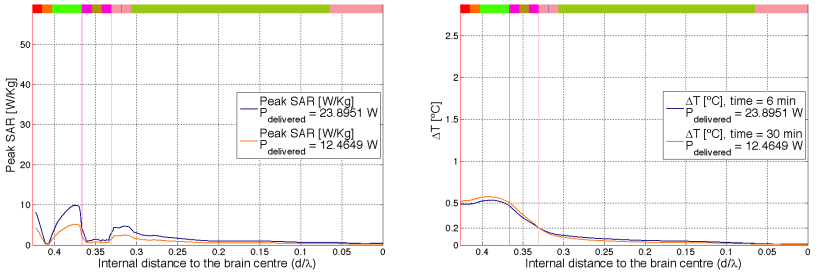

Figure 3: SAR (up) and temperature increase (down) for the temple setting.

The natural electromagnetic helmet also seems to act as a thermo-insulator, since it warms up as much as the outer tissue but maintains the temperature gradient in the brain small and within safe regimes. Therefore, we can conclude that we are in the presence of a natural and dynamic electromagnetic and thermal shield that protects our brain to non-harsh exposure.

This conclusion is to be taken within its limitations, due to the range of parameters analyzed through this research together with the simplifications involved in the modeling of a realistic human head. In particular, there are many

factors to be accounted for in the employed thermoregulatory model, such as sweating, panting, variable heat loss in lungs, capillarity, vasodilatation, variable blood flow or metabolism, clothing, circadian rhythm or even alterations in the thermoregulatory response itself due to temperature increase in the hypothalamus provided by the deposited RF energy, etc. With the powerful computing resources available today, however, it is not risky envisaging the possibility of reducing current scientific uncertainties for human exposure to electromagnetic fields by using the human thermal response. The use of hybrid models brings new possibilities to deliver more accurate basic restrictions to this safety levels. The adoption of a basic restriction directly involving the temperature increase with different reference levels for the various parts of the body according to their sensitivity to heat, in combination to already existing SAR-based limits would bring more precise data for the human-EMF exposure scenario. Future research includes the determination of the avalanche effect that breaks the protective nature of the skull, which may be strongly dependent upon the employed thermoregulatory model.

5. Acknowledgment

The authors would like to thank Fundación Séneca, the science and technology agency in the Region of Murcia, Spain, for partly funding this research under the 05746/PI/07 project.

References

[1] IEC 62209-1, Human exposure to radio frequency fields from hand-held and body-mounted wireless communication devices – Human models, instrumentation, and procedures – Part 1: Procedure to determine the specific absorption rate (SAR) for hand-held devices used in close proximity to the ear (frequency range of 300 MHz to 3 GHz), 2005.

[2] International Commission on Non-Ionizing Radiation Protection (ICNIRP) Guidelines, Guidelines for limiting exposure to time-varying electric, magnetic, and electromagnetic fields (up to 300 GHz), Health Physics 74 (4): 494-522; 1998.

[3] Adair, E. R., Adams, B. W., Akel, G. M., Minimal changes in hypothalamic temperature accompany microwave-induced alteration of thermoregulatory behavior, Bioelectromagnetics, vol. 5, pp. 13-30, 1984.

[4] Mason, P. A., et al., Recent advances in dosimetry measurements and modeling, in Radio Frequency Radiation Dosimetry, B. J. Klauenberg and D. Miklavèiè, Eds. Norwell, MA, Kluwer, Springer, 2000, pp. 141-155.

[5] Ghandi, O. P. et al., Electromagnetic absorption in the human head and neck for mobile telephones at 835 and 1900 MHz, IEEE Transactions on Microwave Theory and Techniques, Vol. 44, No. 10, pp. 1865-1873, 1996.

[6] CENELEC EN50383: Basic standard for the calculation and measurement of electromagnetic field strength and SAR related to human exposure from radio base stations and fixed terminal stations for wireless telecommunication systems (110 MHz–40 GHz), 2002.

[7] Joseph, W. and Martens, L., Safety factor for determination of occupational electromagnetic exposure in phantom model, Electronics Letters, Vol. 39, No. 23, pp. 1663-1664, 2003.

[8] Christ, A. et al., The dependence of electromagnetic far-field absorption on body tissue composition in the frequency range from 300 MHz to 6 GHz, IEEE Transactions on Microwave Theory and Techniques, Vol. 54, No. 5, pp. 2188-2195, 2006.

[9] Bernardi, P., et al., SAR Distribution and Temperature Increase in an Anatomical Model of the Human Eye Exposed to the Field Radiated by the User Antenna in a Wireless LAN, IEEE Transactions on Microwave Theory and Techniques, Vol. 46, No. 12, 1998.

[10] Gabriel, C., Compilation of the dielectric properties of body tissues at RF and microwave frequencies, Brooks Air Force, Brooks AFB, TX, Tech. Rep. AL/OE-TR-1996-0037, 1996.

[11] Pennes, H. H., Analysis of tissue and arterial blood temperature in the resting human forearm, Journal of Applied Physiology, Vol. 1, pp. 93-102, 1948.

[12] Adair, E. R. et al., Thermophysiological responses of human volunteers during controlled whole-body ratio frequency exposure at 450 MHz, Bioelectromagnetics, vol. 19, pp. 232-245, 1998.